NOTES AND CORRESPONDENCE

Can Global Warming Strengthen the East Asian Summer Monsoon?

JIANPING LI

State Key Laboratory of Numerical Modeling for Atmospheric Sciences and Geophysical Fluid Dynamics, Institute of Atmospheric Physics, Chinese Academy of Sciences, Beijing, China

ZHIWEI WU

Meteorological Research Division, Environment Canada, Dorval, Quebec, Canada

ZHIHONG JIANG AND JINHAI HE

Key Laboratory of Meteorological Disaster of Ministry of Education, Nanjing University of Information Science and Technology, Nanjing, China

(Manuscript received 16 September 2009, in final form 25 August 2010)

ABSTRACT

The Indian summer monsoon (ISM) tends to be intensified in a global-warming scenario, with a weakened linkage with El Niño–Southern Oscillation (ENSO), but how the East Asian summer monsoon (EASM) responds is still an open question. This study investigates the responses of the EASM from observations, theoretical, and modeling perspectives. Observational and theoretical evidence demonstrates that, in contrast to the dramatic global-warming trend within the past 50 years, the regional-mean EASM rainfall is basically dominated by considerable interannual-to-decadal fluctuations, concurrent with enhanced precipitation over the middle and lower reaches of the Yangtze River and over southern Japan and suppressed rainfall amount over the South China and Philippine Seas. From 1958 through 2008, the EASM circulation exhibits a southward shift in its major components (the subtropical westerly jet stream, the western Pacific Ocean subtropical high, the subtropical mei-yu–baiu–changma front, and the tropical monsoon trough). Such a southward shift is very likely or in part due to the meridional asymmetric warming with the most prominent surface warming in the midhigh latitudes (45°–60°N), which induces a weakened meridional thermal contrast over eastern Asia. Another notable feature is the enhanced ENSO–EASM relationship within the past 50 years, which is opposite to the ISM. Fourteen state-of-the-art coupled models from the Intergovernmental Panel on Climate Change show that the EASM strength does not respond with any pronounced trend to the global-warming ''A1B'' forcing scenario (with an atmospheric CO_2 concentration of 720 ppm) but shows interannual-to-decadal variations in the twenty-first century (2000–99). These results indicate that the primary response of the EASM to a warming climate may be a position change instead of an intensity change, and such position change may lead to spatial coexistence of floods and droughts over eastern Asia as has been observed in the past 50 years.

1. Introduction

Quite a few studies have suggested that the Indian summer monsoon (ISM) tends to be intensified in association with a weakened relationship with El Niño–Southern Oscillation (ENSO) in a greenhouse warming scenario. Meehl and Washington (1993) found the final equilibrium of ISM precipitation is likely to increase with increased carbon dioxide (CO_2). Kitoh et al. (1997) and Hu et al. (2000) obtained similar results from different models. Although the explanations for such a phenomenon are still controversial, larger thermal gradient and increased moisture transport are believed to be two principal factors responsible for the enhanced ISM. Kumar et al. (1999) and Hu et al. (2000) revealed that increased surface air temperatures Ts over Eurasia

Corresponding author address: Dr. Jianping Li, State Key Laboratory of Numerical Modeling for Atmospheric Sciences and Geophysical Fluid Dynamics, Institute of Atmospheric Physics, Chinese Academy of Sciences, P.O. Box 9804, Beijing 100029, China.
E-mail: ljp@lasg.iap.ac.cn

DOI: 10.1175/2010JCLI3434.1

in winter and spring may favor the enhanced land–ocean thermal gradient conducive to a strong ISM. Meehl and Arblaster (2003) and Ueda et al. (2006) suggested that a larger moisture flux convergence resulting from a warming Indian Ocean leads to the intensification of the mean rainfall. Ashrit et al. (2001) indicated that an enhancement of the thermal gradient as well as intensified moisture conditions over the ISM region contributes to the weakening of the effect of warm ENSO events on the monsoon.

As the other principal component of the Asian monsoon system, how the East Asian summer monsoon (EASM) responds to a global-warming climate is still an open question. The EASM is distinct from the ISM in many aspects (Ding 1992; Chen 1994; Lau and Yang 1997; Chang 2004; Wang et al. 2008). For rainfall, the EASM often exhibits complex space and time structures. The rainfall variability usually differs between extratropical and tropical eastern Asia (EA) (e.g., Wu and Chen 1998; Zhang et al. 2003; Wu et al. 2006a; R. Wu et al. 2009). The extratropical rainfall is basically connected with the mei-yu–baiu–changma front, whereas the tropical rainfall is highly relevant to the tropical monsoon trough, another primary component of the EASM systems (Zhu et al. 1986; Tao and Chen 1987). Most previous studies on global warming and the EA summer climatic change focus more on some certain areas in EA (e.g., Houghton et al. 2001; Xu 2001; Hu et al. 2003; Wu et al. 2006b,c; Zhu et al. 2007). Menon et al. (2002) investigated the climate effect of black carbon aerosols in China with a general circulation model and found black carbon aerosols may contribute to increased summer floods in southern China and increased drought in northern China. Their numerical experiments excluded the effect of increasing greenhouse gases and consequently simulated a strong cooling tendency in northern China, which is opposite to the observation (see Fig. 2A in Menon et al. 2002). Kimoto (2005) suggested that the extratropical mei-yu–baiu–changma rainfall tends to be intensified in a global-warming scenario based on simulations from a high-resolution version of the Center for Climate System Research (CCSR)/National Institute for Environmental Studies (NIES)/Frontier Research Center for Global Change (FRCGC) and an ensemble of 17 state-of-the-art models. However, if the tropical EA is focused on, the conclusion will be just the opposite, because the tropical monsoon trough rainfall is usually out of phase with the extratropical mei-yu–baiu–changma variations (Zhang et al. 2003; Hirota et al. 2005; Wu et al. 2006a). In addition to the above mentioned things, circulations need to be considered together with precipitation in terms of measuring the strength of the EASM, because the EASM has unique characteristics in both rainfall distribution and associated large-scale circulation systems (Wang et al. 2008).

The contemplation discussed in the previous paragraphs motivated us to examine the long-term variations of the EASM strength from two perspectives, namely, precipitation and circulations. This study attempts to answer whether the EASM is intensified under a global-warming background. How would the EASM respond to a global-warming forcing? Section 2 describes the datasets, models, and method employed in this study. Section 3 presents the observed warming trend and variations of precipitation and circulations over EA. Section 4 analyzes the observed relationship between EASM and ENSO. To verify further the conclusion derived from the observations, the response of the EASM to global-warming forcing is investigated with the ''A1B'' stabilization experiments (with an atmospheric CO_2 concentration of 720 ppm) for the twenty-first century (2000–99) conducted by 14 coupled models (section 5). The last section summarizes major findings and discusses some outstanding issues.

2. Data, model, and method

The main datasets employed in this study include 1) monthly precipitation data from the precipitation reconstruction dataset over land (PREC/L; Chen et al. 2002); 2) Ts data from the University of East Anglia Climatic Research Unit (CRU; Jones et al. 1999); 3) 40-yr European Centre for Medium-Range Weather Forecasts Re-Analysis (ERA-40) data (Uppala et al. 2005) and ERA-interim reanalysis datasets; and 4) the improved extended reconstructed sea surface temperature (SST), version 2 (ERSST V2; Smith and Reynolds 2004).

Global-warming A1B stabilization experiments (with an atmospheric CO_2 concentration of 720 ppm) for the twenty-first century (2000–99) used in this study are conducted by 14 state-of-the-art ocean–atmosphere general circulation models that participated in the 2007 Fourth Assessment Report (AR4) coordinated by the Intergovernmental Panel on Climate Change (IPCC). The 14 models include the

1) Goddard Institute for Space Studies Model E-H (GISS-EH),
2) Institute of Atmospheric Physics Flexible Global Ocean–Atmosphere–Land System Model, gridpoint version 1.0 (IAP FGOALS-g1.0),
3) Institute of Numerical Mathematics Coupled Model, version 3.0 (INM-CM3.0),
4) L'Institut Pierre-Simon Laplace Coupled Model, version 4 (IPSL CM4),
5) Model for Interdisciplinary Research on Climate 3.2, medium-resolution version (MIROC3.2-medres),

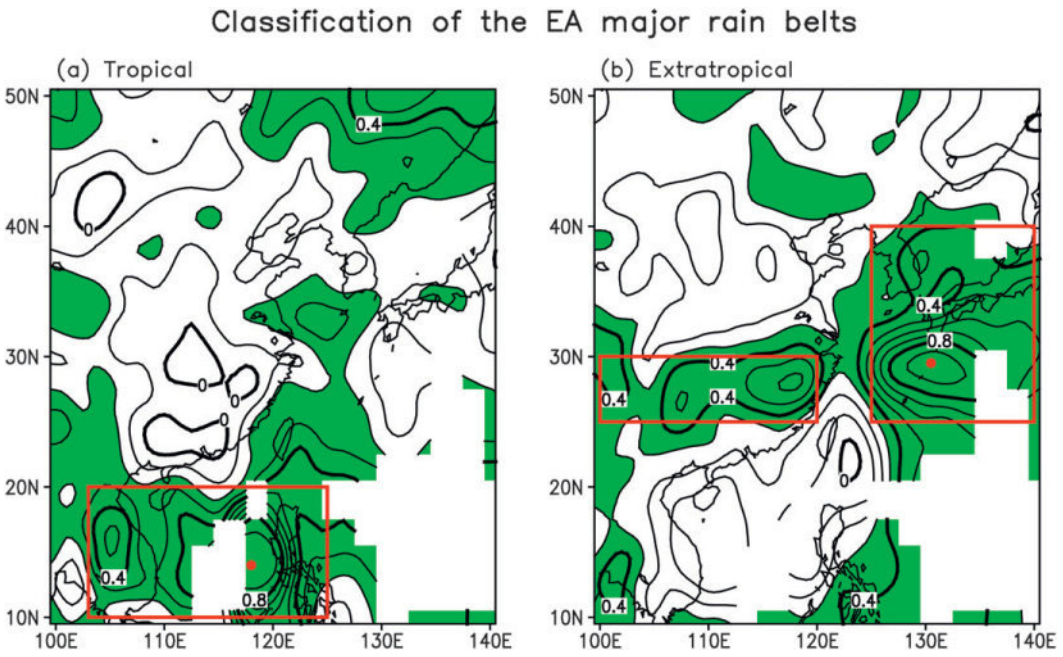

FIG. 1. One-point correlation between precipitation at the (a) tropical and (b) extratropical base points (red dots) and other grids in EA. Shaded areas denote those correlation coefficients that exceed the 95% confidence level. The averaged precipitation in the red boxes at (a) 10°–20°N, 103°–125°E and at (b) 25°–30°N, 100°–120°E + 25°–40°N, 125°–140°E is used to represent the tropical monsoon trough rainfall and subtropical mei-yu–baiu–changma front rainfall, respectively.

6) Meteorological Institute of the University of Bonn, ''ECHO-G'' Model (MIUBECHOG),
7) Max Planck Institute (MPI) ''ECHAM5''/Max Planck Institute Ocean Model (MPI-OM),
8) Meteorological Research Institute Coupled General Circulation Model, version 2.3.2 (MRI CGCM2.3.2),
9) third climate configuration of the Met Office Unified Model (HadCM3),
10) Bjerknes Centre for Climate Research Bergen Climate Model, version 2.0 (BCCR-BCM2.0),
11) Canadian Centre for Climate Modelling and Analysis Coupled General Circulation Model, version 3.1 [CCCma CGCM3.1(T63)],
12) Centre National de Recherches Météorologiques Coupled Global Climate Model, version 3 (CNRM-CM3),
13) Commonwealth Scientific and Industrial Research Organisation, Mark version 3.5 (CSIRO Mk3.5), and
14) Geophysical Fluid Dynamics Laboratory Climate Model, version 2.1 (GFDL CM2.1).

The primary data used in this study cover the period from 1958 to 2008. We employed ERA-40 data for the period 1958–2002 and extended the data from 2003 to 2008 by using ERA-interim reanalysis data. To maintain temporal homogeneity, the 2003–08 ERA-interim data were adjusted by removing the climatological difference between the ERA-40 and ERA-interim datasets (Wang et al. 2010). The horizontal resolution of the ERA interim was interpolated to 2.5° × 2.5°.

To quantify the tropical monsoon trough rainfall and the subtropical mei-yu–baiu–changma front rainfall of the EASM, we use the classification method of precipitation area given by Ting and Wang (1997). From the standard deviations of the summer precipitation over EA for the 1958–2008 period, we select two grids that are of the largest rainfall variance over the tropical and extratropical EA, respectively, as two base points (red dots in Fig. 1). On the basis of the one-point correlation map of the summer precipitation between the two base points, and the other grids over EA (Fig. 1), we then use the mean precipitation in the red box areas, which are of the same rainfall variability as the two base points, to represent the EASM tropical and extratropical rainfall variations, respectively.

To derive the dominant modes of the EASM, we use multivariate EOF analysis (MV-EOF) on a set of three meteorological fields in June–August (JJA), including precipitation and 850-hPa winds. The MV-EOF analysis method was described in detail in Wang (1992); it has the advantage of capturing spatial phase relationships among the various circulation and precipitation fields.

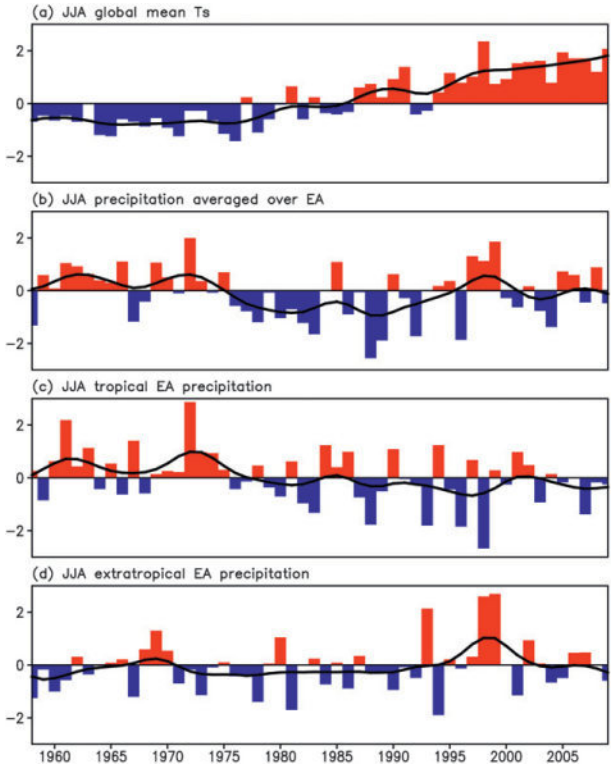

FIG. 2. (a) JJA normalized global mean Ts (color bars) from the CRU observation (Jones et al. 1999) for 1958–2009. JJA normalized precipitation (color bars) averaged over (b) EA, (c) tropical EA, and (d) subtropical EA. The thick black curves denote decadal variations obtained using a nine-point Gaussian-type low-pass filter.

In this paper, a correlation coefficient matrix is constructed to eliminate geographic difference. As such, the eigenvectors (spatial patterns) are nondimensional.

3. Observed EASM variations in a global-warming background

Figure 2a shows the JJA global mean Ts. It displays a pronounced warming trend during the 1958–2009 period, being relatively cooler before 1979 and warmer after 1980. Such a trend exceeds the 99.9% confidence level (Hereinafter, the periods before and after 1979 are treated as cool and warm epochs, respectively, for the following composite analysis). In contrast to such a significant global-warming trend, the mean precipitation over EA does not show notable trends for the 1958–2009 period but does show pronounced interannual-to-decadal variations (Fig. 2b). Note that if one focuses on the period from the 1960s through the early 1990s, a notable drought trend does exist. As mentioned in section 1, the summer rainfall primarily exhibits an opposite long-term variation tendency between the tropical monsoon trough rainfall and the subtropical mei-yu–baiu–changma (Figs. 2c,d). The former decreases significantly, exceeding the 95% confidence level, whereas the latter has a slightly increasing trend. It indicates that the tropical monsoon trough has weakened and the subtropical mei-yu–baiu–changma has strengthened in the past 50 years. If both the subtropical mei-yu–baiu–changma and the tropical monsoon trough rainfall are considered to be the EASM rainfall, then the mean precipitation over the two regions does not show notable trends within the past five decades but rather pronounced interannual-to-decadal variations (Fig. 2b). The conclusion derived from the observed land-based rainfall is basically consistent with the 20 EASM indices summarized by Wang et al. (2008). Each of these indices can depict the EASM system, both its tropical and subtropical components, from their individual aspect. It is interesting to find that none of these indices bears a notable increasing (or decreasing) trend but all show considerable interannual-to-decadal variations (not shown), which is in favor of the result from Fig. 2b. These observational facts can hardly support the notion that the EASM has strengthened or weakened within the past decades despite that regional droughts or floods do exist in the EA domain. Then, how does the EASM respond to a warming climate?

To answer the above question, we need to examine the interdecadal change of the dominant mode of the EASM within the past decades. Figure 3 presents the leading mode of the EASM for the 1958–79 (cool) and 1980–2008 (warm) periods. A prominent feature is that the precipitation absolute-value centers corresponding to the subtropical mei-yu–baiu–changma rainfall are located basically north of 30°N during 1958–79, whereas such absolute-value centers shift southward, with the center located around 30°N, during 1980–2008. At the same time, the precipitation absolute-value centers associated with the tropical monsoon trough also move southward. Coupled with the precipitation variations, the anticyclonic wind anomalies accompanied by the western Pacific subtropical high (WPSH) withdraw southwestward from the cool epoch through the warm epoch, with enhanced southwesterly winds prevailing over southern China. The southward shift of the leading mode of the EASM rainfall and circulations from the cool epoch through the warm epoch enhances the rainfall amount over the middle and lower reaches of the Yangtze River Valley and southern Japan and suppresses precipitation over the South China Sea (SCS) and Philippine Sea.

Although the first leading modes explain only a small portion (10%–20%) of the total variance of rainfall and 850-hPa winds because of the complexity of the EASM spatial patterns, they are physically meaningful. The major components of the EASM, such as the WPSH, the

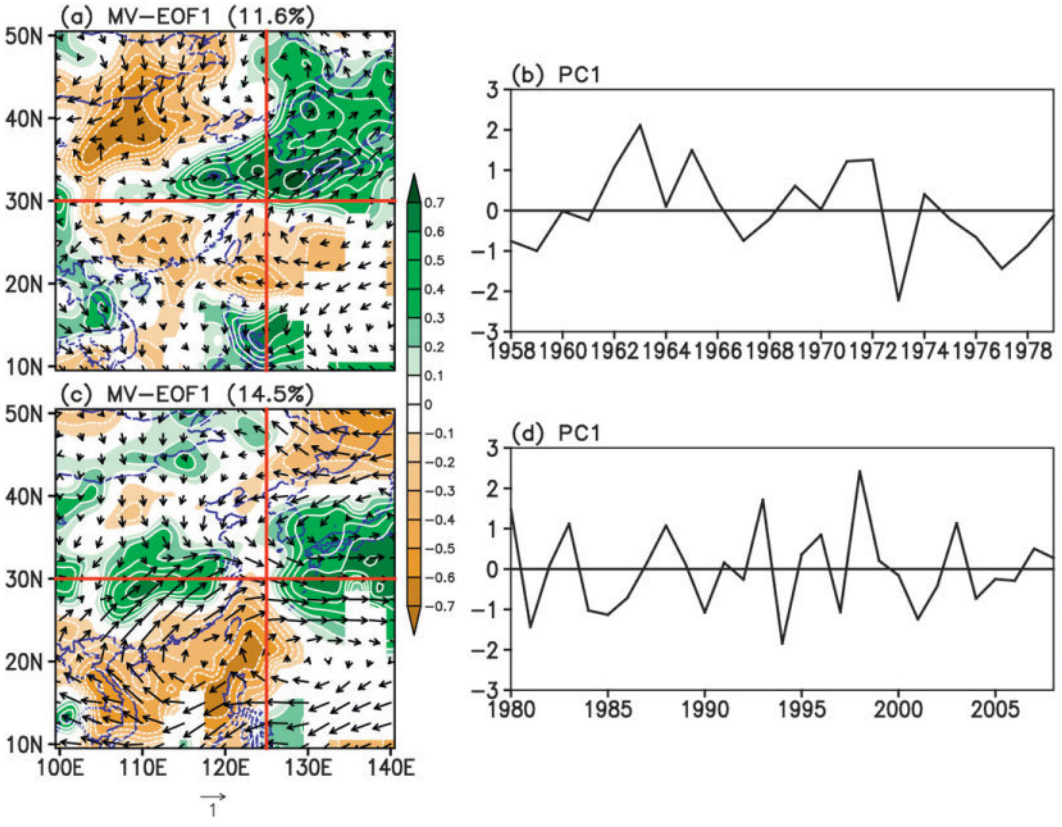

FIG. 3. Spatial patterns of the leading MV-EOF mode of the EA summer precipitation (color shadings) and 850-hPa winds (vectors) for the (a) 1958–79 and (c) 1980–2008 periods, and the (b),(d) corresponding principal components (PC). All quantities are nondimensional because they were derived from the correlation coefficient matrix.

tropical monsoon trough, and the mei-yu–baiu–changma, are clearly depicted by the first modes (Fig. 3; e.g., Wang et al. 2008). On the other hand, because the first leading modes are not statistically separable from the other high leading modes according to the rule given by North et al. (1982), it indicates that the other high leading modes may share features that are similar to those that the first leading modes bear. These results highlight the necessity of investigating the interdecadal change in the first leading mode.

One important question needing to be answered is how global warming drives such a change of the EASM. Figure 4 presents the composite difference of 200-hPa JJA winds and 500-hPa geopotential heights *H* between the 1958–79 and 1980–2008 periods over EA (the latter minus the former). A noticeable feature is that large areas of positive *H* anomalies associated with anticyclonic wind anomalies prevail over northern EA. The northern flank of climatological westerly jets over EA (color shadings in Fig. 4) is basically controlled by anomalously easterly winds, whereas the southern flank is primarily controlled by anomalously westerly winds. Such wind anomalies tend to shift the EA subtropical jets more southward than normal. Meanwhile, the WPSH also withdraws southward. Large areas of positive 500-hPa *H* anomalies occupy the Philippine Sea and SCS, while the East China Sea, Korean Peninsula, and Japan Islands and the adjacent oceans are controlled by negative 500-hPa *H* anomalies. Coupled with such circulation changes, the subtropical rain belt shifts southward and brings more precipitation over the middle and lower reaches of the Yangtze River while precipitation over the SCS and Philippine Sea is suppressed (Figs. 3a,c).

Considering that circulation changes are usually intimately coupled with the low boundary forcing anomalies, it is reasonable to speculate that the interdecadal change of the EASM systems may be related to the interdecadal change in the low boundary forcing. It can be clearly seen from Fig. 5 that the EA warming is not spatially uniform. The maximum warming areas are basically located in the mid–high latitudes of EA (45°–60°N) with the warming amplitude decreasing southeastward (Fig. 5a). Such a warming pattern generates a Ts gradient from north to south (Fig. 5b). In the meantime, the

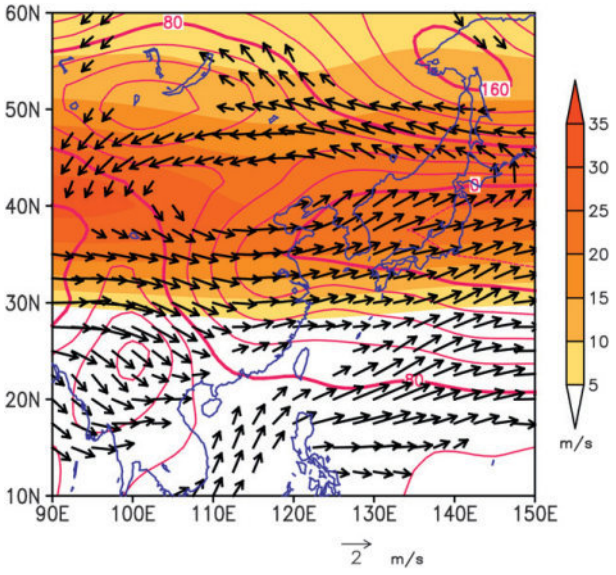

FIG. 4. Composite difference of JJA 200-hPa winds (vectors; m s^{-1}) and geopotential heights (contours; m) between the 1958–79 and 1980–2008 periods over EA (the latter minus the former). Color shadings denote 200-hPa JJA climatological westerly jets (m s^{-1}).

Ts gradient produced by the mid–high latitudes warming maximum is opposite to that produced by the solar radiation whose direction is from south to north. It consequently leads to a weakened meridional thermal contrast and decreased meridional pressure gradient in the mid–high latitudes. This can physically explain why the EA 200-hPa westerly jet stream decelerates in its northern flank and tends to move southward (Webster and Yang 1992; Yang et al. 2002). On the other hand, the cyclonic vorticity trend is significant from east China to southern Japan, where the climatological WPSH is located. The result here suggests that the southward retreat of the WPSH may be in part a result of the prominent warming over northern EA.

The following presents the theoretical evidence that the primary response of the EASM to global warming is the southward shift of the WPSH and the associated monsoon circulation systems. First, we define the central axis (or high ridge axis) of a given high pressure system as the connection line of centers at each level. At each center point, we have $(\partial z/\partial y)_p = 0$, where z denotes the geopotential height and y denotes the meridional direction. Therefore, along the high ridge axis, we get the following formula:

$$\delta\left(\frac{\partial z}{\partial y}\right)_p = \left(\frac{\partial}{\partial y}\right)_p\left(\frac{\partial z}{\partial y}\right)_p \delta y + \frac{\partial}{\partial p}\left(\frac{\partial z}{\partial y}\right)_p \delta p = 0.$$

According to the static equation and the state equation,

$$\frac{\partial}{\partial p}\left(\frac{\partial z}{\partial y}\right)_p = \left(\frac{\partial}{\partial y}\right)_p\left(\frac{\partial z}{\partial p}\right) = \frac{1}{\rho^2 g}\left(\frac{\partial \rho}{\partial y}\right)_p \quad \text{and}$$

$$\left(\frac{\partial \rho}{\partial y}\right)_p = -\frac{\rho}{T}\left(\frac{\partial T}{\partial y}\right)_p.$$

The slope k of the high ridge axis meets the following relationship:

$$k \equiv \left(\frac{\partial y}{\partial z}\right) = -\frac{1}{T}\left(\frac{\partial T}{\partial y}\right)_p \Bigg/ \left(\frac{\partial^2 z}{\partial y^2}\right)_p. \tag{1}$$

According to Eq. (1), for the high ridge axis, $(\partial^2 z/\partial y^2)_p < 0$, the axis tilts to the warm side. Therefore, under the meridional asymmetric heating anomaly forcing (Fig. 5), the axis of the WPSH tends to tilts northward, which in the upper troposphere decelerates the EA 200-hPa westerly jet stream in its northern flank and shifts it southward. Since the WPSH and westerly jet stream are dynamically coupled, the WPSH in the mid- and lower troposphere also exhibits a southward shift.

To summarize, the primary response of the EASM to the global warming is the southward shift of the main rain belts and the associated circulation systems (the westerly jet stream, the WPSH, and the subtropical front and the tropical monsoon trough). No significant trend is detected in its strength. These systemic changes are very likely or in part induced by the meridional asymmetric warming over EA.

4. EASM and ENSO

In contrast to the weakened ISM–ENSO relationship in a global-warming scenario, the EASM tends to have a strengthened linkage with ENSO. To investigate the relationship between the EASM and ENSO, first we need to quantitatively measure the strength of the EASM. Here, we employ the monsoon index defined by Li and Zeng (2002; hereinafter I_{LZ}). This monsoon index has good performance in depicting the EASM (Wang et al. 2008) and has been adopted by the National Oceanic and Atmospheric Administration to monitor the EASM strength variations (see online at http://www.cpc.noaa.gov/products/Global_Monsoons/Asian_Monsoons/monsoon_index.shtml). The I_{LZ} is based on seasonal alternation in wind direction over monsoon domains. It is defined as

$$I_{LZ} = \frac{\|\overline{\mathbf{V}}_W - \mathbf{V}_i\|}{\|\overline{\mathbf{V}}\|} - 2, \tag{2}$$

where $\overline{\mathbf{V}}_W$ and $\mathbf{V}_i$ are the climatological winter wind vector as the reference state (here averaged from 1968 to

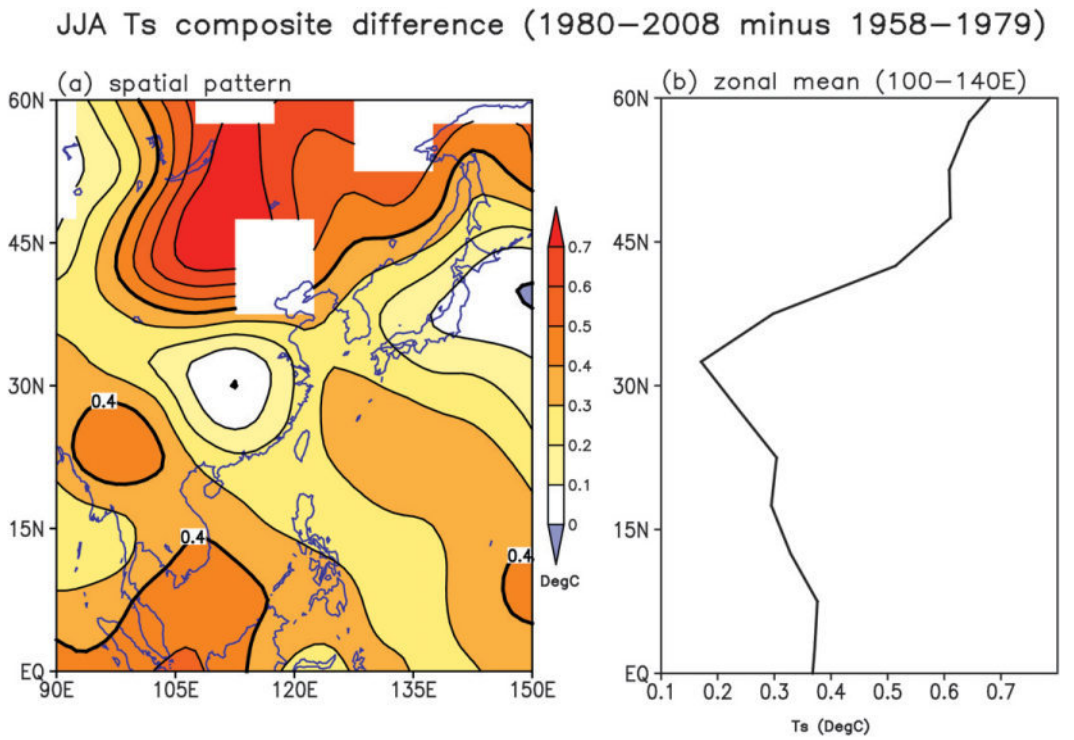

FIG. 5. JJA Ts composite difference between the 1958–79 and 1980–2008 periods over EA (the latter minus the former): (a) spatial pattern (color shadings and contours; °C) and (b) zonal mean averaged over the EA section (100°–140°E) (black curve; °C).

1996) and monthly wind vectors at a point, respectively, and $\overline{\mathbf{V}} = (\overline{\mathbf{V}}_W + \overline{\mathbf{V}}_S)/2$ is the climatological mean wind vector. Here $\overline{\mathbf{V}}_S$ is the climatological summer wind (for the Northern Hemisphere, taking $\overline{\mathbf{V}}_W = \overline{\mathbf{V}}_{\text{Jan}}$ and $\overline{\mathbf{V}}_S = \overline{\mathbf{V}}_{\text{Jul}}$; for the Southern Hemisphere, taking $\overline{\mathbf{V}}_W = \overline{\mathbf{V}}_{\text{Jul}}$ and $\overline{\mathbf{V}}_S = \overline{\mathbf{V}}_{\text{Jan}}$). The norm $\|A\|$ is defined as

$$\|A\| = \left(\iint_S |A|^2 \, dS \right)^{1/2},$$

where here S now denotes the domain of integration. In calculations at a point (i, j),

$$\left\|A_{i,j}\right\| \approx \Delta s \left[\left(\left|A^2_{i-1,j}\right| + 4\left|A^2_{i,j}\right| + \left|A^2_{i+1,j}\right| \right) \cos\varphi_j + \left|A^2_{i,j-1}\right| \cos\varphi_{j-1} + \left|A^2_{i,j+1}\right| \cos\varphi_{j+1} \right]^{1/2} \quad (3)$$

where $\Delta s = a\Delta\varphi\Delta\lambda/4$, $\Delta\varphi$ and $\Delta\lambda$ (radians) are resolutions in the meridional and zonal directions, respectively, a is the mean radius of the earth, and ϕ_j is the latitude at the point (i, j). The I_{LZ} is an extension of the static normalized seasonality monsoon index, which is defined by $\|\overline{\mathbf{V}}_1 - \overline{\mathbf{V}}_7\|/\|\overline{\mathbf{V}}\|$, that was presented by Zeng et al. (1994); 2 is subtracted on the right-hand side of Eq. (2) because the critical value of significance of the quantity $\|\overline{\mathbf{V}}_1 - \overline{\mathbf{V}}_7\|/\|\overline{\mathbf{V}}\|$ is 2 (Li and Zeng 2000).

It is well known that the EASM experiences strong interannual variations associated with ENSO (e.g., Webster and Yang 1992; Chang et al. 2000; Wang et al. 2000, 2008; Wu and Wang 2000; Wu et al. 2003; Lau and Nath 2006). However, the relationship between the EASM and ENSO is not stationary (Wu and Wang 2002; Lee et al. 2010). One piece of such evidence is seen from the amplitude of the monsoon index, I_{LZ} having increased considerably since 1980 (not shown). Wavelet analysis of the I_{LZ} time series indicates that the oscillation period of the EASM also shifted from 4–5 yr before 1979 to quasi biennial after 1980 (not shown). This is consistent with some previous studies (Shen and Lau 1995; Miao and Lau 1990; Nitta and Hu 1996). Nitta and Hu (1996) found that the quasi-biennial oscillation signal becomes stronger after the mid-1970s in their first principal component of summer temperature or rainfall.

Figure 6 provides robust evidence that the relationship between the EASM and ENSO has strengthened within the past decades. Figure 6a shows an intimate linkage between the EASM and the eastern Pacific SST anomalies prior to the summer monsoon season. For the cool period of 1958–79, the correlation between I_{LZ} and

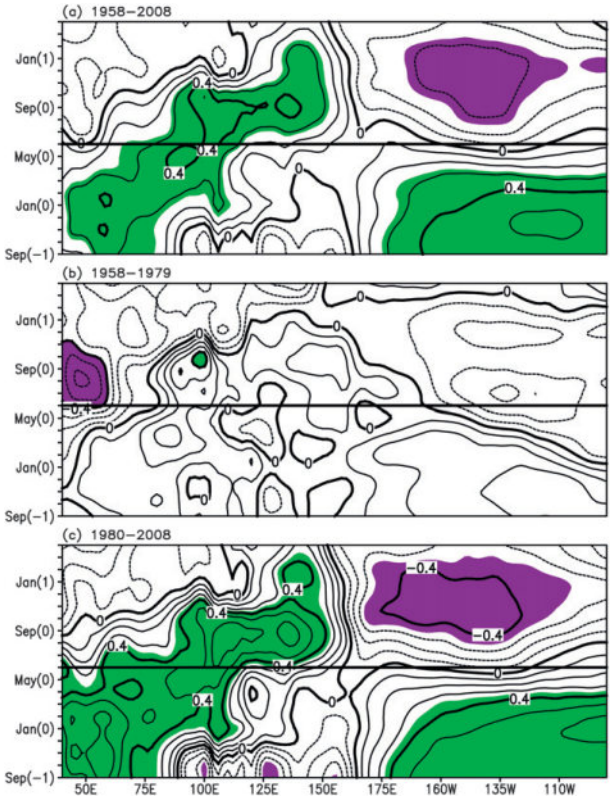

FIG. 6. The lead/lag correlation coefficients between I_{LZ} (Li and Zeng 2002) and the SST anomalies averaged between −5°S and 5°N from September(−1) to April(1) for (a) 1958–2008, (b) 1958–79, and (c) 1980–2008. The thick horizontal line indicates July(0), where the simultaneous correlations are shown. Here, the −1, 0, and 1 in parentheses indicate the previous year, the current year, and the following year, respectively. The green (purple) areas are significantly positive (negative) correlation areas, exceeding the 95% confidence level.

the eastern Pacific SST anomalies is weak (Fig. 6b), yet it becomes strong for the warm period of 1980–2008 (Fig. 6c). A similar feature has been observed between the SCS summer monsoon and ENSO (Wang et al. 2009). While the EASM displays a strengthened connection with the eastern Pacific SST anomalies, it also exhibits an enhanced linkage with SST anomalies in the equatorial Indian Ocean and with those in the SCS (Figs. 6b,c), consistent with Ding et al. (2009). In light of the fact that SST anomalies in the equatorial Indian Ocean and the SCS are highly relevant to ENSO, all of these observations indicate that the relationship between the EASM and ENSO has been strengthened since the late 1970s. This is different from the ISM, whose relationship with ENSO has been weakened within the past decades.

Under a warming climate background, the EASM does not show any pronounced trends in its strength, but the connection between the EASM and ENSO is enhanced. This may imply that ENSO is still a principal predictor for EASM future change.

5. Future change of the EASM

In a global-warming scenario, how would the EASM change in the next 100 years? To answer this question, we present responses of the EASM strength variations in A1B stabilization experiments (with an atmospheric CO_2 concentration of 720 ppm) for the twenty-first century (2000–99), produced by 14 state-of-the-art ocean–atmosphere general circulation models that participated in the 2007 AR4 coordinated by the IPCC. Driven by this forcing condition, all models display a pronounced Ts warming trend in the twenty-first century (not shown). It indicates that all models successfully yield a global-warming background. Concurrent with such a warming-trend forcing, none of these models responds with any notable strengthening or weakening trends in the long-term EASM variations (not shown). All models, including the multimodel ensemble mean, basically exhibit considerable interannual-to-interdecadal variations. People may argue that these models have discrepancy not only in simulating current climate but also in projecting future change. However, if it is true that the multimodel results are more believable than one model result, then the above future projections will further verify our assumption that global warming cannot make the EASM stronger or weaker, which is consistent with what has been observed in the past 50 years.

6. Summary and discussion

Although global warming brings about many pronounced changes of the global climate (e.g., Lau et al. 2008), what kind of influences it may exert on regional climate is still controversial. This work focuses on EASM responses to a meridional asymmetric warming climate with the maximum surface warming center over northern EA. Observed evidence, theoretical verification, and numerical experiment results do not support the notion that the EASM tends to get stronger or weaker under such a surface warming forcing. The primary response of the EASM is the southward shift in the major rain belts and the associated circulations. On account of such a southward shift, the middle and lower reaches of the Yangtze River Valley and southern Japan are getting wetter and the SCS and the Philippine Sea are getting drier. It contributes to the spatial coexistence of droughts and floods over EA, yet the mean precipitation over EA remains with no increasing or decreasing trend (Zhu et al. 2007). Such a rainfall-belt southward shift is intimately connected with the changes in the subtropical

westerly jet stream and the WPSH. In addition, the EASM does not weaken its connection with ENSO as the ISM does in a warming climate. On the contrary, its linkage with ENSO has been enhanced in the past 50 years, which makes ENSO remain as a crucial predictor for the EASM future change.

However, it is still not clear whether the enhancement of the linkage between EASM and ENSO is due to global warming. If so, how does it work? If not, what factors contribute to the strengthened EASM–ENSO relationship? Besides global warming, other physical processes may contribute to the interdecadal change of the EASM (Baldwin et al. 2003; Yu et al. 2004; He et al. 2006; Z. Wu et al. 2009). These outstanding issues need further investigation. Some of them will be discussed in other papers.

Acknowledgments. The authors acknowledge the reviewers' helpful and important comments. The authors are also thankful for stimulating discussions with Dr. Fei-fei Jin. The first two authors acknowledge the support of the National Basic Research Program "973" (Grant 2010CB950400). Zhiwei Wu is also supported by the Special Research Program for Public Welfare (Meteorology) of China under Grant GYHY200906016 and by the Sustainable Agriculture Environment Systems (SAGES) research initiative of Agriculture and Agri-Food Canada through the Natural Sciences and Engineering Research Council of Canada (NSERC) fellowship program.

REFERENCES

Ashrit, R. G., K. R. Kumar, and K. K. Kumar, 2001: ENSO–monsoon relationships in a greenhouse warming scenario. *Geophys. Res. Lett.,* **28,** 1727–1730.

Baldwin, M. P., D. W. J. Thompson, E. F. Shuckburgh, W. A. Norton, and N. P. Gillett, 2003: Weather from the stratosphere. *Science,* **301,** 317–319.

Chang, C.-P., 2004: Preface. *East Asian Monsoon,* C.-P. Chang, Ed., Series on Meteorology of East Asia, Vol. 2, World Scientific, v–vi.

——, Y. S. Zhang, and T. Li, 2000: Interannual and interdecadal variations of the east Asian summer and tropical Pacific SSTs. Part I: Roles of the subtropical ridge. *J. Climate,* **13,** 4310–4325.

Chen, G. T.-J., 1994: Large-scale circulations associated with the east Asian summer monsoon and the mei-yu over south China and Taiwan. *J. Meteor. Soc. Japan,* **72,** 959–983.

Chen, M., P. Xie, J. E. Janowiak, and P. A. Arkin, 2002: Global land precipitation: A 50-yr monthly analysis based on gauge observations. *J. Hydrometeor.,* **3,** 249–266.

Ding, R. Q., K.-J. Ha, and J. Li, 2009: Interdecadal shift in the relationship between the east Asian summer monsoon and the tropical Indian Ocean. *Climate Dyn.,* **34,** 1059–1071, doi:10.1007/s00382-009-0555-2.

Ding, Y.-H., 1992: Summer monsoon rainfalls in China. *J. Meteor. Soc. Japan,* **70,** 397–421.

He, J., Z. Wu, Z. Jiang, C. Maio, and G. Han, 2006: "Climate effect" of the northeast cold vortex and its influences on meiyu. *Chin. Sci. Bull.,* **51,** 2803–2809.

Hirota, N., M. Takahashi, N. Sato, and M. Kimoto, 2005: Recent climate trends in the east Asia during the baiu season of 1979–2003. *SOLA,* **1,** 137–140.

Houghton, J. T., Y. Ding, D. J. Griggs, M. Noguer, P. J. van der Linden, X. Dai, K. Maskell, and C. A. Johnson, Eds., 2001: *Climate Change 2001: The Scientific Basis*. Cambridge University Press, 881 pp.

Hu, Z.-Z., M. Latif, E. Roeckner, and L. Bengtsson, 2000: Intensified Asian summer monsoon and its variability in a coupled model forced by increasing greenhouse gas concentrations. *Geophys. Res. Lett.,* **27,** 2681–2684.

——, S. Yang, and R. Wu, 2003: Long-term climate variations in China and global warming signals. *J. Geophys. Res.,* **108,** 4614, doi:10.1029/2003JD003651.

Jones, P. D., M. New, D. E. Parker, S. Martin, and I. G. Rigor, 1999: Surface air temperature and its variations over the last 150 years. *Rev. Geophys.,* **37,** 173–199.

Kimoto, M., 2005: Simulated change of the east Asian circulation under global warming scenario. *Geophys. Res. Lett.,* **32,** L16701, doi:10.1029/2005GL023383.

Kitoh, A., S. Yukimoto, A. Noda, and T. Motoi, 1997: Simulated changes in the Asian summer monsoon at times of increased atmospheric CO_2. *J. Meteor. Soc. Japan,* **75,** 1019–1031.

Kumar, K. K., B. Rajagopalan, and M. A. Cane, 1999: On the weakening relationship between Indian monsoon and ENSO. *Science,* **284,** 2156–2159.

Lau, K.-M., and S. Yang, 1997: Climatology and interannual variability of the Southeast Asian summer monsoon. *Adv. Atmos. Sci.,* **14,** 141–162.

Lau, N.-C., and M. J. Nath, 2006: ENSO modulation of the interannual and intraseasonal variability of the east Asian monsoon—A model study. *J. Climate,* **19,** 4508–4530.

——, A. Leetmaa, and M. J. Nath, 2008: Interactions between the responses of North American climate to El Niño–La Niña and to the secular warming trend in the Indian–western Pacific Oceans. *J. Climate,* **21,** 476–494.

Lee, S.-S., P. N. Vinayachandran, K.-J. Ha, and J.-G. Jhun, 2010: Shift of peak in summer monsoon rainfall over Korea and its association with El Niño–Southern Oscillation. *J. Geophys. Res.,* **115,** D02111, doi:10.1029/2009JD011717.

Li, J., and Q. C. Zeng, 2000: Significance of the normalized seasonality of wind field and its rationality for characterizing the monsoon. *Sci. China,* **43,** 646–653.

——, and ——, 2002: A unified monsoon index. *Geophys. Res. Lett.,* **29,** 1274, doi:10.1029/2001GL013874.

Meehl, G. A., and W. M. Washington, 1993: South Asian summer monsoon variability in a model with doubled atmospheric carbon dioxide concentration. *Science,* **260,** 1101–1104.

——, and J. M. Arblaster, 2003: Mechanisms for projected future changes in south Asian monsoon precipitation. *Climate Dyn.,* **21,** 659–675.

Menon, S., J. Hansen, L. Nazarenko, and Y. Luo, 2002: Climate effects of black carbon aerosols in China and India. *Science,* **297,** 2250–2253, doi:10.1126/science.1075159.

Miao, J. H., and K.-M. Lau, 1990: Interannual variability of east Asian monsoon rainfall. *Quart. J. Appl. Meteor.,* **1,** 377–382.

Nitta, T., and Z.-Z. Hu, 1996: Summer climate variability in China and its association with 500 hPa height and tropical convection. *J. Meteor. Soc. Japan,* **74,** 425–445.

North, G. R., T. L. Bell, R. F. Cahalan, and F. J. Moeng, 1982: Sampling errors in the estimation of empirical orthogonal functions. *Mon. Wea. Rev.,* **110,** 699–706.

Shen, S., and K.-M. Lau, 1995: Biennial oscillation associated with the east Asian summer monsoon and tropical sea surface temperatures. *J. Meteor. Soc. Japan,* **73,** 105–124.

Smith, T. M., and R. W. Reynolds, 2004: Improved extended reconstruction of SST (1854–1997). *J. Climate,* **17,** 2466–2477.

Tao, S., and L.-X. Chen, 1987: A review of recent research on the east Asian summer monsoon in China. *Monsoon Meteorology, Monogr. Geol. Geophys.,* Vol. 7, Oxford University Press, 60–92.

Ting, M. F., and H. Wang, 1997: Summer time U.S. precipitation variability and its relation to Pacific sea surface temperature. *J. Climate,* **10,** 1853–1873.

Ueda, H., A. Iwai, K. Kuwako, and M. E. Hori, 2006: Impact of anthropogenic forcing on the Asian summer monsoon as simulated by eight GCMs. *Geophys. Res. Lett.,* **33,** L06703, doi:10.1029/2005GL025336.

Uppala, S. M., and Coauthors, 2005: The ERA-40 Re-Analysis. *Quart. J. Roy. Meteor. Soc.,* **131,** 2961–3012.

Wang, B., 1992: The vertical structure and development of the ENSO anomaly mode during 1979–1989. *J. Atmos. Sci.,* **49,** 698–712.

——, R. Wu, and X. Fu, 2000: Pacific–east Asian teleconnection: How does ENSO affect east Asian climate? *J. Climate,* **13,** 1517–1536.

——, Z. Wu, J. Li, J. Liu, C.-P. Chang, Y. Ding, and G. Wu, 2008: How to measure the strength of the east Asian summer monsoon? *J. Climate,* **21,** 4449–4463.

——, F. Huang, Z. Wu, J. Yang, X. Fu, and K. Kikuchi, 2009: Multi-scale climate variability of the South China Sea monsoon: A review. *Dyn. Atmos. Oceans,* **47,** 15–37.

——, Z. Wu, J. Liu, C.-P. Chang, J. Li, and T.-J. Zhou, 2010: Another look at interannual-to-interdecadal variations of the east Asian winter monsoon: The northern and southern temperature modes. *J. Climate,* **23,** 1495–1512.

Webster, P. J., and S. Yang, 1992: Monsoon and ENSO: Selectively interactive systems. *Quart. J. Roy. Meteor. Soc.,* **118,** 877–926.

Wu, R., and L. Chen, 1998: Decadal variation of summer rainfall in the Yangtze-Huaihe River Valley and its relationship to atmospheric circulation anomalies over east Asia and western North Pacific. *Adv. Atmos. Sci.,* **15,** 510–522.

——, and B. Wang, 2000: Interannual variability of summer monsoon onset over the western North Pacific and the underlying processes. *J. Climate,* **13,** 2483–2501.

——, and ——, 2002: A contrast of the east Asian summer monsoon–ENSO relationship between 1962–77 and 1978–93. *J. Climate,* **15,** 3266–3279.

——, Z.-Z. Hu, and B. P. Kirtman, 2003: Evolution of ENSO-related rainfall anomalies in east Asia. *J. Climate,* **16,** 3742–3758.

——, Z. Wen, S. Yang, and Y. Li, 2009: An interdecadal change in southern China summer rainfall around 1992-93. COLA Tech. Rep. 281, 34 pp.

Wu, Z., Z. Jiang, and J. He, 2006a: The comparison analysis of flood and droughts features among the first flood period in South China, Meiyu period in the Yangtze River and Huaihe River Valleys and rainy season in north China in the last 50 years (in Chinese). *Chin. J. Atmos. Sci.,* **30,** 391–401.

——, J. Li, J. He, and Z. Jiang, 2006b: Large-scale atmospheric singularities and summer long-cycle droughts-floods abrupt alternation in the middle and lower reaches of the Yangtze River. *Chin. Sci. Bull.,* **51,** 2027–2034.

——, ——, ——, and ——, 2006c: Occurrence of droughts and floods during the normal summer monsoons in the mid- and lower reaches of the Yangtze River. *Geophys. Res. Lett.,* **33,** L05813, doi:10.1029/2005GL024487.

——, B. Wang, J. Li, and F.-F. Jin, 2009: An empirical seasonal prediction model of the east Asian summer monsoon using ENSO and NAO. *J. Geophys. Res.,* **114,** D18120, doi:10.1029/2009JD011733.

Xu, Q., 2001: Abrupt change of the mid-summer climate in central east China by the influence of atmospheric pollution. *Atmos. Environ.,* **35,** 5029–5040.

Yang, S., K.-M. Lau, and K.-M. Kim, 2002: Variations of the east Asian jet stream and Asian–Pacific–American winter climate anomalies. *J. Climate,* **15,** 306–325.

Yu, R., B. Wang, and T. Zhou, 2004: Tropospheric cooling and summer monsoon weakening trend over east Asia. *Geophys. Res. Lett.,* **31,** L22212, doi:10.1029/2004GL021270.

Zeng, Q., B. Zhang, Y. Liang, and S. Zhao, 1994: The Asian summer monsoon—A case study. *Proc. Indian Natl. Sci. Acad.,* **60A,** 81–96.

Zhang, Q. Y., S. Y. Tao, and L. T. Chen, 2003: The interannual variability of east Asian summer monsoon indices and its association with the pattern of general circulation over east Asia (in Chinese). *Acta Meteor. Sin.,* **61,** 559–568.

Zhu, Q., J. He, and P. Wang, 1986: A study of circulation differences between east-Asian and Indian summer monsoons with their interaction. *Adv. Atmos. Sci.,* **3,** 466–477.

Zhu, X., J. He, and Z. Wu, 2007: Meridional seesaw-like distribution of the meiyu rainfall over the Changjiang-Huaihe River Valley and characteristics in the anomalous climate years. *Chin. Sci. Bull.,* **52,** 2420–2428.